Tolerancing analysis taking into account thermomechanical strains

Laurent Pierre, Denis Teissandier, Jean-Pierre Nadeau

Tolerancing analysis taking into account thermomechanical strains

Laurent Pierre [1], Denis Teissandier [2], Jean Pierre Nadeau [1]

(1) : Arts et Métiers ParisTech
TREFLE, UMR 8508
Esplanade des Arts et Métiers
33405 Talence Cedex - France
Phone/Fax: 33-5-56845428/5436
E-mail: {laurent.pierre, jean-pierre.nadeau}@bordeaux.ensam.fr

(2) : Université de Bordeaux
LMP, UMR 5469
351, cours de la Libération
33405 Talence Cedex - France
Phone/Fax: 33-5-40006220/6964
E-mail: denis.teissandier@u-bordeaux1.fr

Abstract: To improve the performance of a helicopter turboshaft engine requires optimising the energy yield of the different components, and more particularly controlling clearance between the tips of the high pressure turbine blades and the stator. Dimension-chain tools take into account the manufacturing dispersion of the parts and assembly defects. This ensures the interchangeability of the different components and guarantees that a turbine can carry out different service functions, as the turbine is modelled in infinitely rigid solids. However, this approach does not take thermomechanical effects into account. And yet, the different operating regimes of a helicopter engine make it indispensable that the effects caused by the thermodynamic cycle should be integrated. The aim of this article is to show how using dimension chain and thermomechanical tools can contribute to controlling clearances at the tip of a high pressure turbine blade.
Key words: geometric tolerancing; thermomechanics

1- Introduction

Controlling the behaviour and the energy yield of helicopter engines for each of the different operating regimes is indispensable in order to guarantee that the desired power is produced. One way to improve the performance of these turboshaft engines is to optimize the energy yield of the different constituent parts, and in particular to control clearance between the tips of the high pressure turbine blades and the stator.
To achieve this, a geometric tolerancing procedure has to be carried out during the design cycle of a turboshaft engine.
The hypothesis on which the 3D dimension-chain simulation tools are commonly based is that the different parts are modelled as infinitely rigid solids. However, using this approach, it is not possible to take thermomechanical effects into account.
To compensate for this shortcoming, this article proposes a method by which the strain of the parts subjected to thermal flux can be taken into account in the 3D dimension-chain calculations.
Several studies have been carried out to manage compliant structure: [JC1], [SC1], [SL1] and [XW1]. These works take into account geometric variations induced by the assembly process and manufacturing dispersions. In this article, one hypothesis is that the assembly process deals with infinitely rigid solids. The geometric variations caused by the thermodynamic cycle are integrated in the different behaviours of a turboshaft engine.
In the first part, the physical hypothesis associated with this study are stated to introduce two different behaviours of the system studied: a rigid behaviour situation where the parts are considered as infinitely rigid, and a thermomechanical behaviour situation, associated with a thermal flux which could potentially modify the contacts and distort the geometry of the parts. Changes in contacts from rigid behaviour to thermomechanical behaviour are taken into account and also the strain on the parts themselves. In the second part, an application of this work to a sub-unit in a high pressure turbine of a helicopter engine is demonstrated. In this paper, the used tolerance analysis tool is an application of deviation hulls and clearance hulls [F1], [GD1] and the used thermomechanical calculation tool is Samcef. Lastly, after setting out the main conclusions, the future prospects for this work are presented.

2- Tolerancing analysis taking into account thermomechanical strains

The geometric models used in 3D dimension-chains are generally based on the following hypotheses: no form default in real surfaces, no local strain in surfaces in contact and no deformable parts.

Two different behaviours will be considered for every system studied:
- rigid behaviour: all parts are at 20°C and are considered as being infinitely rigid.
- thermomechanical behaviour: some parts are subjected to thermomechanical stresses. Thermomechanical strains on the parts are then taken into account in the 3D dimension chains.

The problem was restricted to those systems where the topological structure of the contact graphs (or of the joints) in rigid behaviour and thermomechanical behaviour remain the same. This means that there is no supplementary joint and no suppression of a joint between the two behaviours. On the other hand, a joint defined by different parameters (minimal clearance, maximal clearance, nature of contact …) may change.

2.1- Rigid behaviour: dimension-chain of infinitely rigid solids

2.1.1 Modelling the geometrical defects in a part

Real surfaces are modelled by substituted surfaces [BB1]. A substituted surface is an ideal surface (i.e. geometrically perfect) of the same type as the nominal surface of which it is a particular physical representation. This is described in figure 1, which illustrates the three different types of modelling used in tolerancing: the nominal model (CAD model), the skin model and the substituted surfaces model.

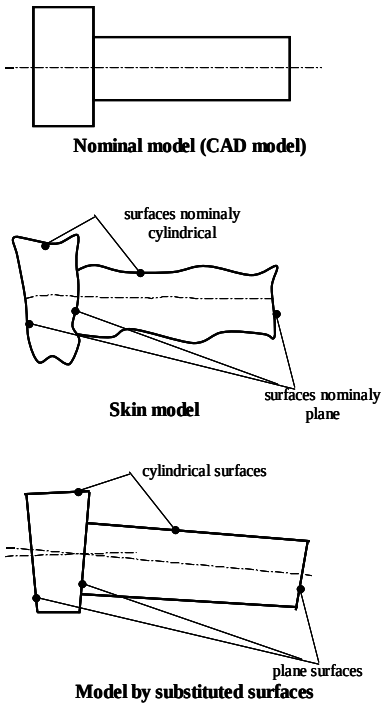

Figure 1: Geometric modelling of a real surface.

The nominal model is the one used in a geometric modeller: it is by definition geometrically perfect. The skin model provides a representation of the real surfaces of the part and acts as a graphic support for expressing geometric specifications [DB1]. The skin model of the shaft consists of three real surfaces: one is nominally plane and two are nominally cylindrical. Lastly, the substituted surface model consists of three surfaces: one plane and two cylindrical. The geometric defects of a real surface are defined by the relative position between a substituted surface and the corresponding nominal surface. Figure 2 illustrates the defaults of the relative position of the substituted surfaces designated by 1,1; 1,2 and 1,3 of the shaft 1.
Each surface is designated by a pair of numbers: 1,2 refers to (substituted) surface 2 of part 1. Surfaces 1,1n; and 1,2n 1,3n refer respectively to the nominal surfaces corresponding to surfaces 1,1; 1,2 and 1,3.

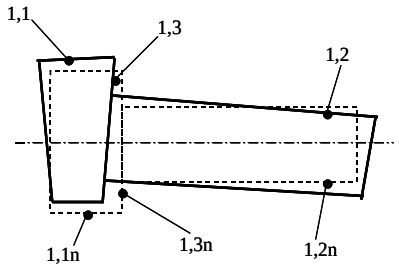

representation by substituted surfaces

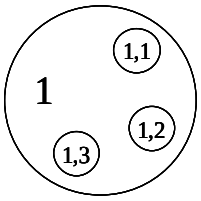

representation by a graph

Figure 2 : Relative position of two substitution surfaces of a part.

Figure 2 shows part 1 (large circle) in diagram form and also shows surfaces 1,1; 1,2 and 1,3 (small circles). This acts as a graphic support to show the structure of a mechanism on which one can visualise the dimension-chains [BM1].
Observe $\left[d_{1,1/1,2}\right]$ position deviations between surfaces 1,1 and 1,2. Position deviations between surfaces 1,2 and 2,2, which are still called simply geometric deviations, characterise the geometric defaults of surfaces 1,1 and 1,2. When modelling these deviations using substituted surfaces it is not possible to take into account the form defaults of surfaces 1,1 and 1,2.
$\left[d_{1,1/1,2}\right]$ can be formalised mathematically by a small displacement torsor [BB1], by a matrix [T1], etc. In this article, the small displacement torsor is used [CB1].

The following relations can be written:

$$\left[d_{1,1/1,2}\right]=\left[d_{1,1/1,1n}\right]+\left[d_{1,1n/1,2n}\right]+\left[d_{1,2n/1,2}\right] \qquad (1)$$

Given that by definition the nominal model of a part has no defect, (2) can be expresses as follows :

$$\left[d_{1,1/1,2}\right]=\left[d_{1,2/1,2n}\right]+\left[d_{1,2n/1,2}\right] \qquad (2)$$

2.1.2 Modelling 3D dimension-chains in a mechanism

Let us consider figure 3 : two parts, 1 and 2, are in cylindrical pair type contact via their respective surfaces 1,2 and 2,2 and in ball and plane pair contact via their respective interfaces 1,3 and 2,3. In a diagram, this is represented by two edges linking respectively apexes 1,2 ; 2,2 and 1,3 ; 2,3. Let us suppose that a functional condition (FC) limiting the relative position of surfaces 1,1 and 2,1 must be respected.
This is a condition of coaxiality such that, for every direction orthogonal to the x-axis, the displacement d of point A on the axis of surface 1,1 in relation to the axis of surface 2,1 respects the following equation (see figure 3):

$$d_{min} \le d \le d_{max} \qquad (3)$$

In the diagram, FC is within a rectangle on an edge linking apexes 1,1 and 2,1.

The diagram describing the parts and surfaces of a system and also the joints and the functional condition is commonly called a joint graph or contact graph [BM1].

Here the specifications for coaxiality of 1,1 in relation to 1,2 and of 2,1 in relation to 2,2 on parts 1 and 2 respectively are specifications that impact on the FC. Similarly, diameter specifications for surfaces 1,2 and 2,2 also influence the FC.

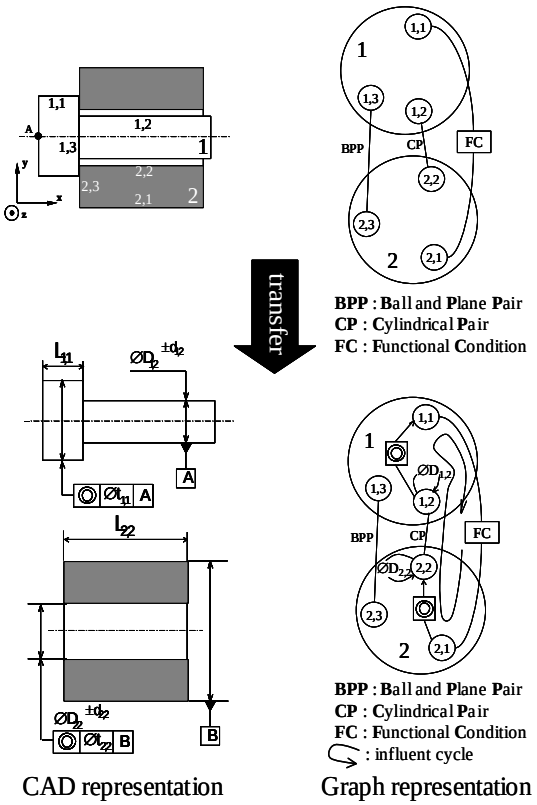

Figure 3 : Transfer of FC.

Generally speaking, the two location specifications and the two diameter specifications are the result of the transfer of FC to parts 1 and 2.

Each one appears on an arc oriented to the circles of parts 1 and 2. The arrow indicates the toleranced element and the origin of the arc indicates the surface of reference. For the diameter specifications, these are specifications that are intrinsic to surfaces 1,2 and 2,2.
The influent specifications, the influent joint (CP) and the FC formalise an influent cycle (see figure 3). Equation (4), justified by the influent cycle, formalises at point A dependences between the FC, the location deviations of parts 1 and 2 and the cylindrical pair joint deviations (between surfaces 1,2 and 2,2) [TC1] :

$$\left[d_{1,1/2,1}\right]=\left[d_{1,1/1,2}\right]+\left[d_{1,2/2,2}\right]+\left[d_{2,2/2,1}\right] \qquad (4)$$

One result here is that the ball and plane pair joint between 1,3 and 2,3 is non-influent on the FC. The deviations of surfaces 1,3 and 2,3 are also non-influent on FC. This means that respect for the FC is independent of any geometrical defaults in surfaces 1,3 and 2,3 and of the ball and plane pair joint between 1,3 and 2,3.

2.1.3 Formalisation of relations between functional condition, geometric specifications and contact specifications

In this article, deviation hulls [GD1] to define the admissible limits for geometrical defaults in a part (defined by a specification) and clearance hulls to define the admissible limits for relative displacements between two surfaces in contact (defined by a clearance) [GS1] will be used.

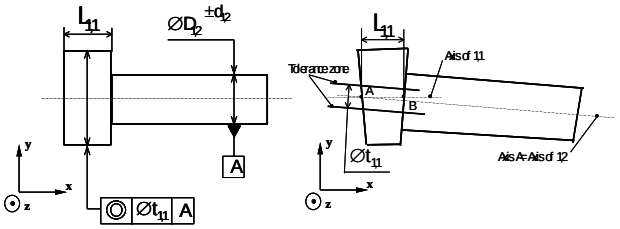

Figure 4 : Definition of a geometric specification with substituted surfaces according to ISO 1101.

Note $\left[\mathrm{d}_{1,1/1,2}\right]$ the Small Displacement Torsor, characterising the relative position of 1,1 in relation to 1,2. In the base $(\mathbf{x},\mathbf{y},\mathbf{z})$ at point A $\left[\mathrm{d}_{1,1/1,2}\right]$ is expressed as follows:

$$\left[\mathrm{d}_{1,1/1,2}\right]_{\mathrm{A}}=\begin{bmatrix}\boldsymbol{\rho}_{1,1,/1,2}\\ \boldsymbol{\varepsilon}_{\mathrm{A},1,1,/1,2}\end{bmatrix} \qquad (5)$$

with $\boldsymbol{\rho}_{1,1,/2,1}\begin{bmatrix}\rho_{,1/1,2x}\\ \rho_{,1/1,2y}\\ \rho_{,1/1,2z}\end{bmatrix}$: rotation vector and $\boldsymbol{\varepsilon}_{\mathrm{A},1,1,/2,1}\begin{bmatrix}\varepsilon_{A,1,1/1,2x}\\ \varepsilon_{A,1,1/1,2y}\\ \varepsilon_{A,1,1/1,2z}\end{bmatrix}$: translation vector at point A.

The deviation hull $\mathsf{D}_{1,1/1,2}$ characterising the coaxiality specification of 1,1 in relation to 1,2 can be written [GD1], [GS1]:

$$\mathsf{D}_{1,1/1,2}=\begin{Bmatrix}\left(\boldsymbol{\varepsilon}_{\mathrm{A},1,1/1,2}.\mathbf{y}\right)^2+\left(\boldsymbol{\varepsilon}_{\mathrm{A},1,1/1,2}.\mathbf{z}\right)^2\le\left(\frac{t_{1,1}}{2}\right)^2\\ \left(\boldsymbol{\varepsilon}_{\mathrm{B},1,1/1,2}.\mathbf{y}\right)^2+\left(\boldsymbol{\varepsilon}_{\mathrm{B},1,1/1,2}.\mathbf{z}\right)^2\le\left(\frac{t_{1,1}}{2}\right)^2\end{Bmatrix} \qquad (6)$$

To simplify the writing of the hulls, the limits of admissible defects in 2D modelling will be studied in the plane $(\mathrm{A},\mathbf{z})$.

$\mathsf{D}_{1,1/1,2}$ can be written::

$$\mathsf{D}_{1,1/1,2}=\begin{Bmatrix}\left(\boldsymbol{\varepsilon}_{\mathrm{A},1,1/1,2}.\mathbf{y}\right)^2\le\left(\frac{t_{1,1}}{2}\right)^2\\ \left(\boldsymbol{\varepsilon}_{\mathrm{B},1,1/1,2}.\mathbf{y}\right)^2\le\left(\frac{t_{1,1}}{2}\right)^2\end{Bmatrix}=\begin{Bmatrix}-\frac{t_{1,1}}{2}\le\boldsymbol{\varepsilon}_{\mathrm{A},1,1/1,2}.\mathbf{y}\le+\frac{t_{1,1}}{2}\\ -\frac{t_{1,1}}{2}\le\boldsymbol{\varepsilon}_{\mathrm{B},1,1/1,2}.\mathbf{y}\le+\frac{t_{1,1}}{2}\end{Bmatrix} \qquad (7)$$

According to the property of the small displacement fields [CB1] (see figure 4) it is possible to deduce:

$$\boldsymbol{\varepsilon}_{\mathrm{B},1,1/1,2}=\boldsymbol{\varepsilon}_{\mathrm{A},1,1/1,2}+\mathbf{BA}\times\boldsymbol{\rho}_{1,1/1,2}\ \text{ with }\ \mathbf{BA}\begin{bmatrix}-L_{1,1}\\ 0\\ 0\end{bmatrix} \qquad (8)$$

Hence with (8) $\mathsf{D}_{1,1/1,2}$ is written at point A:

$$\mathsf{D}_{1,1/1,2}=\begin{Bmatrix}-\frac{t_{1,1}}{2}\le\varepsilon_{\mathrm{A},1,1/1,2y}\le+\frac{t_{1,1}}{2}\\ -\frac{t_{1,1}}{2}\le\varepsilon_{\mathrm{A},1,1/1,2y}+L_{1,1}.\rho_{1,1/1,2z}\le+\frac{t_{1,1}}{2}\end{Bmatrix} \qquad (9)$$

Figure 5 shows a graph of the deviation hull $\mathsf{D}_{1,1/1,2}$ defined by (9). The translation deviation at point A following $\mathbf{y}$ is projected on axis ε_{Ay} and the rotation deviation following $\mathbf{z}$ is projected according to ρ_z. The interior of the hull (boundary included) represents the geometric deviation in conformity with the coaxiality specification (see figure 4) [TD1].

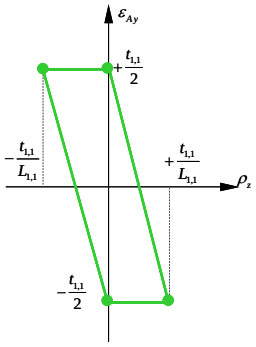

Figure 5 : Deviation hull $D_{1,1/1,2}$ at point A (coaxiality of part 1).

By the same reasoning, the deviation hull $D_{2,2/2,1}$ is determined at point A, which characterises the coaxiality specification for part 2, which is shown following axes ε_{Ay} and ρ_z in figure 6.

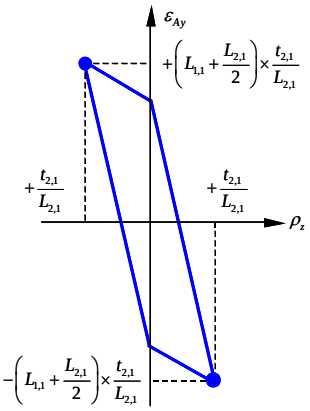

Figure 6 : Deviation hull of coaxiality of part 2 at point A.

Moreover, using a similar method to that used for the deviation hulls, from figure 7, illustrating the clearance of the cylindrical pair joint between surfaces 1,2 and 2,2, the clearance hull $D_{1,2/2,2}$ is defined. The clearance hull $D_{1,2/2,2}$ expressed at point A is represented in figure 8, and given in equation (10).

$$J_{\max}=\left(D_{2,1}+d_{2,1}\right)-\left(D_{1,2}-d_{1,2}\right) \qquad (10)$$

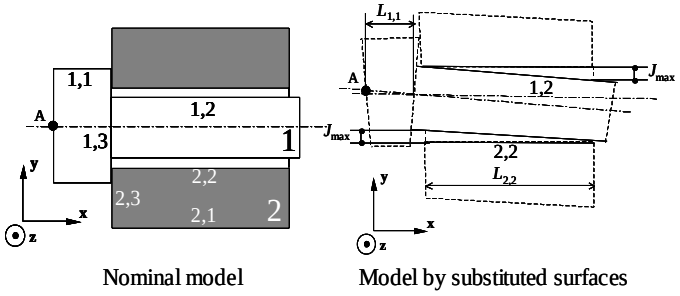

Figure 7 : Definition of a joint with clearance by substituted surfaces

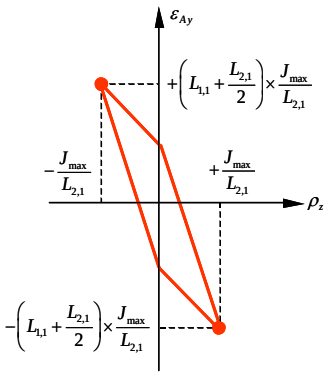

Figure 8 : Clearance hull $D_{1,2/2,2}$ of joint 1,2/2,2 at point A.

Equation (4) is a relation between small displacement torsors. A similar equation (11) can be written for the hulls that correspond to point A. This gives:

$$D_{1,1/2,1}=D_{1,1/1,2}+D_{1,2/2,2}+D_{2,2/2,1} \qquad (11)$$

The sum of two hulls is a Minkowski sum [F1], [MD1], [RL1] and [Z1]. A representation of hull $D_{1,1/2,1}$ expressed at point A is shown in figure 9.
In particular, from this is deduced expression (12) formalising respect for the FC in the worst case in rigid behaviour.

$$\begin{aligned} d_{max} &\geq +\frac{t_{1,2}}{2}+\left(L_{1,1}+\frac{L_{2,1}}{2}\right)\times\left(\frac{t_{2,1}+J_{max}}{L_{2,1}}\right) \\ d_{min} &\leq -\frac{t_{1,2}}{2}-\left(L_{1,1}+\frac{L_{2,1}}{2}\right)\times\left(\frac{t_{2,1}+J_{max}}{L_{2,1}}\right) \end{aligned} \qquad (12)$$

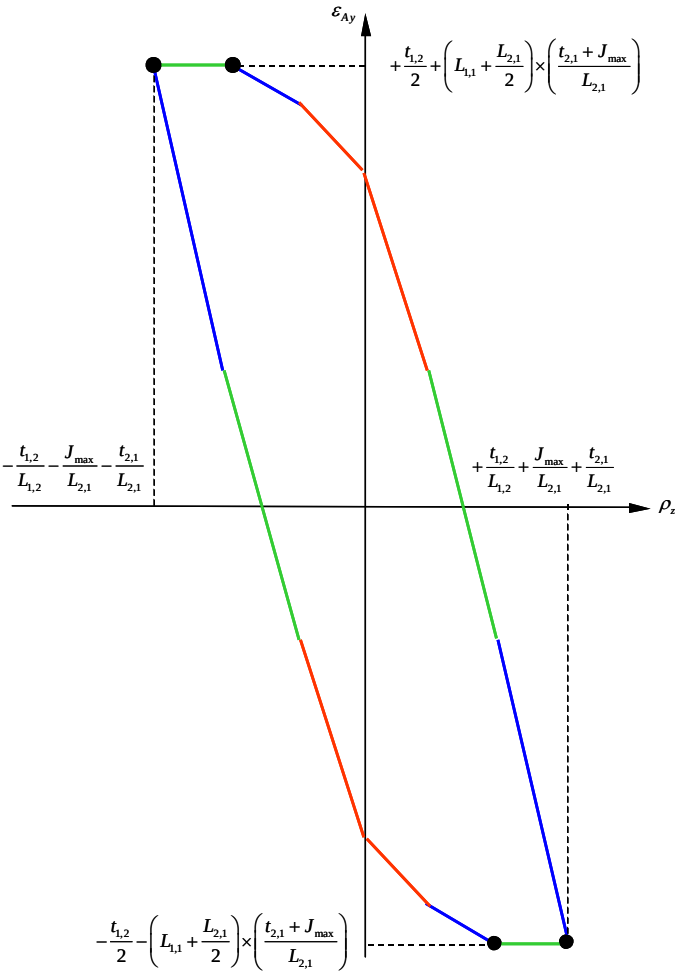

Figure 9 : Minkowski sum illustrating equation (9).

2.2- Thermomechanical behaviour: dimension-chain integrating thermomechanical strains

2.2.1- Physical hypotheses

Let us consider figure 10 showing a system with rigid behaviour and thermomechanical behaviour.
The rigid behaviour of this system was studied in §2.1 where respect for the FC is characterised by (10). Henceforth, it must be ensured that the FC is respected under thermomechanical behaviour. The hypothesis that part 2 remains undeformable is stated: only part 1 is subject to thermomechanical strain.

An other hypothesis is stated: the topological structure of the joint graph in rigid behaviour and all thermomechanical behaviours remains the same. This means that there is no supplementary joint and no suppression of a joint between the two behaviours. The main consequence is that the joints that are influent on the FC remain the same for both behaviours. The influent cycle identified in figure 3 remains the same.
On the other hand, the different parameters that characterise a joint (minimal clearance, maximal clearance and nature of contact) may change. As a result, the thermomechanical strains on the joints and the influent parts will modify the different tolerances which ensure that the FC is respected. By tolerances are more precisely the dimensions of the tolerance zones of coaxiality and the tolerance intervals of the diameters: see figure 11.

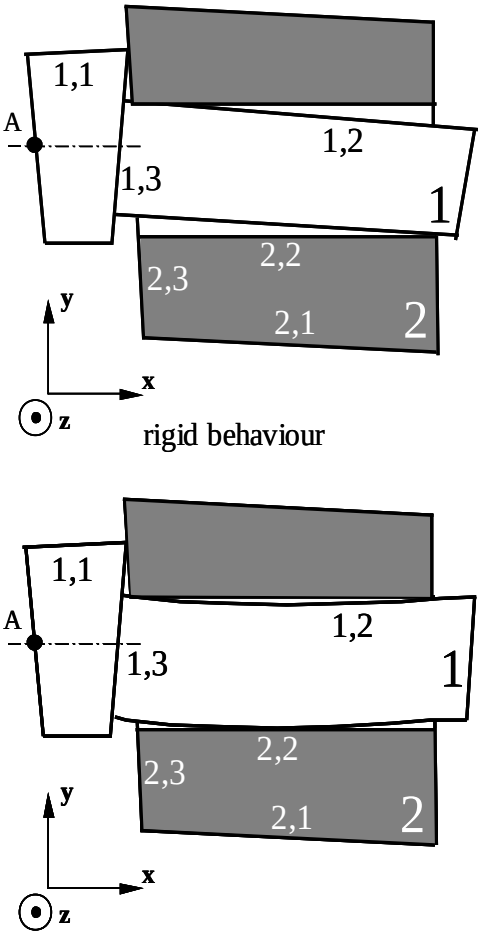

Figure 10 : System behaviour.

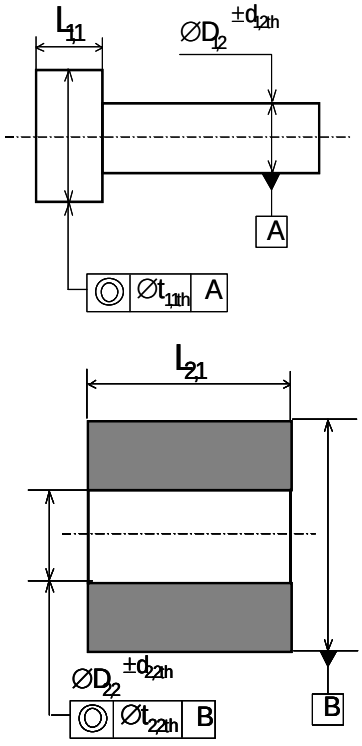

Figure 11 : Specifications for thermomechanical behaviour.

2.2.2- Integration of thermomechanical strains into the joints

A joint can be defined as a set of parameters. Several studies have been carried out on this subject: [DE1], [W1], [SS1] and [DM1]. In this article the definition proposed in [DT1], which is a direct application of that proposed in [DM1] is used.
Thus a joint can be defined by the following parameters:

- type: planar pair, cylindrical pair, ball and cylinder pair, etc.
- situation elements: plane, line, point
- nature: fixed, sliding or floating
- clearance: minimal and maximal clearance: J_{min}, J_{max}.
- forced contact direction: optional

The type of joint conforms to one of the types defined in [I2].
The situation elements position the joint in space, and hence define the axes of the degrees of freedom [CR1], [DT1].
The nature of the contact determines the behaviour of the joint [DM1]:

- Fixed: no displacement is possible (the degrees of freedom are suppressed).
- Sliding: displacements corresponding to the different degrees of freedom are possible, but the surfaces remain in permanent contact one with another. Clearance of the joint is null.
- Floating: displacements corresponding to the different degrees of freedom are possible, and other displacements are limited by clearance.

In the case of a turning pair, cylindrical pair, ball and cylinder pair, spherical pair, or prismatic pair joint clearance is defined as being the difference between the diameter of the hole and the diameter of the shaft. Clearance may be positive, null or negative. In the case of a ball and plane pair, cylinder and plane pair or planar pair, clearance is the distance between the two surfaces potentially in contact. Clearance can then be positive or null: negative clearance has no meaning in physical terms.

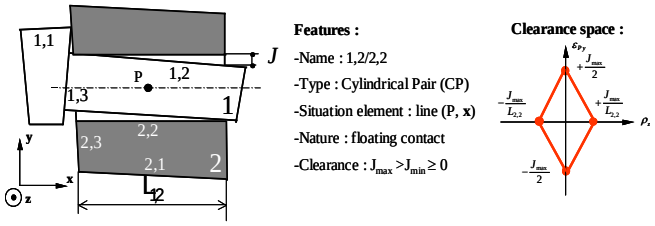

Figure 12 : Cylindrical pair joint in rigid behaviour.

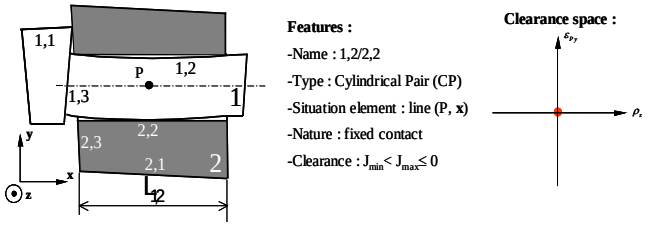

Figure 13 : Cylindrical pair joint in thermomechanical behaviour 1.

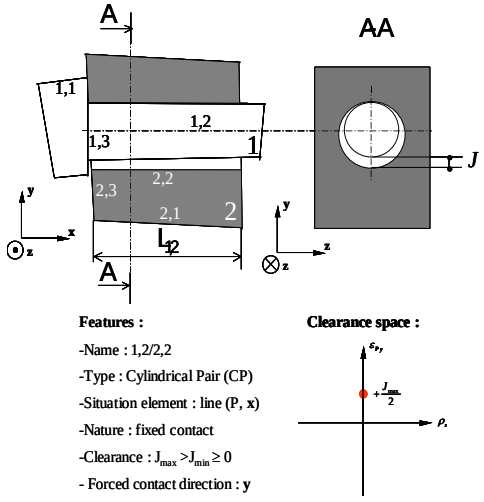

Figure 14 : Cylindrical pair joint in thermomechanical behaviour 2.

A joint is defined in rigid behaviour by a set of parameters that act as reference parameters. Each thermomechanical behaviour will be characterised by a change in the reference parameters for the joint. Only those changes where the type of joint remains invariant are considered.

Figure 12 shows rigid behaviour for the cylindrical pair joint used in figure 3. The situation element is the straight line (P, **x**). The hypothesis that minimal clearance is positive or null is stated. The cylindrical surface 1,2 (shaft) is free to occupy the clearance space in the cylindrical surface 2,2 (hole): the nature of the joint is therefore: floating. The corresponding clearance hull (in the shape of a lozenge at point P, centre of the joint) is also illustrated in figure 12.

In the case of a cylindrical pair joint, all calculations of relative displacements between the two surfaces are carried out from a position of reference where the two surfaces are coaxial.

Let us consider a thermal flux, characteristic of thermomechanical behaviour 1, which expands the diameter of surface 1,2: see figure 13. This expansion is such that maximal clearance is negative or null: surface 1,2 is therefore clamped to surface 2,2. The nature of the joint is therefore: fixed. Surface 1,2 is constrained to be coaxial to surface 2,2: the clearance hull is therefore reduced to a point centred on the origin.

Let us consider a thermal flux, characteristic of thermomechanical behaviour 2, which fixes surface 1,2 by strain in a particular position on surface 2,2: see figure 14. This case defines a forced contact. The minimal clearance of the joint remains strictly positive but surface 1,2 occupies a fixed position in relation to surface 2,2: the two cylindrical surfaces are in contact according to their generatrices so that the greatest distance separating the two surfaces is equal to J following y-axis. y-axis characterises the direction of forced contact. In the case of a forced contact, a supplementary parameter is added to the description of the joint specifying the direction of the forced contact (y-axis in this case). The corresponding clearance hull illustrated in figure 14 is therefore a point that corresponds to null rotation and to a translation of an amount J/2 following y-axis.

The thermomechanical behaviour corresponding to figure 10 corresponds to thermomechanical behaviour 1 in figure 13.

An example of the use of thermomechanical behaviour 2 will be shown in §3 in an industrial application.

2.2.3- Integration of thermomechanical strains in the parts

The surfaces that have undergone thermomechanical strain using substituted surfaces are modelled [PT1]. A thermomechanical simulation tool based on a technique for calculating by finite elements discretises the nominal model of a part into points and determines the displacement of each point. It is thus straightforward to describe a surface strained by a set of points. The substituted surface of a thermomechanically strained surface is a surface obtained by approximation using the least squares technique for this set of points.

Thus the relative position of the thermomechanically strained substituted surface and its nominal model using a small displacements torsor is determined.

From equation (1) and figure 2, equation (13) can be written as follows:

$$\left[d_{1,1/1,2}\right]=\left[d_{1,1/1,1th}\right]+\left[d_{1,1th/1,1n}\right]+\left[d_{1,1n/1,2n}\right] + \left[d_{1,2n/1,2th}\right]+\left[d_{1,2th/1,2}\right] \qquad (13)$$

Surfaces 1,1th and 2,2th are the substituted surfaces for the thermomechanically strained surfaces. Torsors $\left[d_{1,1th/1,1n}\right]$ and $\left[d_{1,2th/1,2n}\right]$ characterise the deviations of the relative position of surfaces 1,1th and 2,2th respectively in relation to the nominal surfaces 1,1n and 1,2n.

Given that the nominal model of a part is by definition without defect and without strain, (14) can be written as follows:

$$\left[d_{1,1/1,2}\right]=\left[d_{1,1/1,1th}\right]+\left[d_{1,1th/1,1n}\right]+ \left[d_{1,2n/1,2th}\right]+\left[d_{1,2th/1,2}\right] \qquad (14)$$

(14) can be expressed as follows:

$$\left[d_{1,1/1,2}\right]=\left[d_{1,1/1,2}\right]_{ma}+\left[d_{1,1/1,2}\right]_{th} \quad (15)$$

where:

$$\left[d_{1,1/1,2}\right]_{ma}=\left[d_{1,1/1,1th}\right]+\left[d_{1,2th/1,2}\right] \quad (16)$$

$$\left[d_{1,1/1,2}\right]_{th}=\left[d_{1,1th/1,1n}\right]+\left[d_{1,2n/1,2th}\right] \quad (17)$$

Equation (16) characterises the geometric deviations of surface 1,1 in relation to surface 1,2 that derive from defects in manufacture.
Equation (17) characterises the geometric deviations of surface 1,1 in relation to surface 1,2 that derive from thermomechanical strains.
When considering equation (2) the following hypothesis is stated:

$$\left[d_{1,1/1,2}\right]_{ma}=\left[d_{1,1/1,2}\right] \text{ defined in rigid behaviour} \quad (18)$$

Let us suppose that:

$$\left[d_{1,1/1,2}\right]_{th,A}=\begin{bmatrix}\boldsymbol{\rho}_{1,1,/1,2th}\\ \boldsymbol{\varepsilon}_{A,1,1,/1,2th}\end{bmatrix}$$

with : (19)

$$\boldsymbol{\rho}_{1,1,/1,2th}\begin{bmatrix}\rho_{1,1/1,2thx}\\ \rho_{1,1/1,2thy}\\ \rho_{1,1/1,2thz}\end{bmatrix} \text{ and } \boldsymbol{\varepsilon}_{1,1,/1,2th}\begin{bmatrix}\varepsilon_{A,1,1/1,2thx}\\ \varepsilon_{A,1,1/1,2thy}\\ \varepsilon_{A,1,1/1,2thz}\end{bmatrix}$$

According to the deviation hull defined at point A in §2.1.3 for rigid behaviour, the deviation hull $D_{1,1/1,2}$ for thermodynamic behaviour described in figure 10 by the Minkowski sum (20) is defined as follows:

$$D_{1,1/1,2}=D_{1,1/1,2th}+D_{1,1/1,2ma} \quad (20)$$

with :

$D_{1,1/1,2ma}=D_{1,1/1,2}$ defined in rigid behaviour

$D_{1,1/1,2th}$ is a hull reduced to a point corresponding to the thermomechanical strain defined in (17): see figure 15.

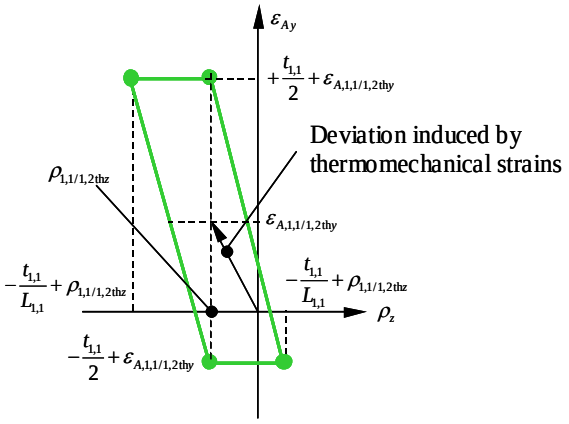

Figure 15 : Deviation hull integrating thermomechanical strains.

2.2.4- Synthesis: formalisation of relations between functional condition, geometric specifications and contact specifications

Equation (11) characterises the dependency between the functional condition, the geometric specifications and the contact specifications by a Minkowski sum for hulls under rigid behaviour. This equation remains valid for thermomechanical behaviour, given the conservation hypothesis for the topological structure of the contact graph shown in §2.2.1.

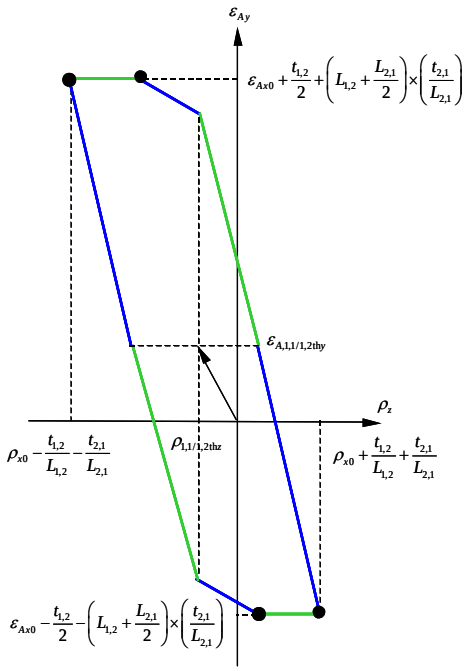

Figure 16 : Minkowski sum illustrating equation (11) with thermomechanical behaviour in figure 10.

Hull $D_{1,1/2,1}$ at point A corresponding to the thermomechanical behaviour represented in figure 10 will be determined, taking into account the deviation hull $D_{1,1/1,2}$ and the clearance hull $D_{1,2/2,2}$ integrating the thermomechanical strains illustrated in figures 15 and 13 respectively and the deviation hull $D_{2,2/2,1}$ illustrated in figure 6, since part 2 is considered as being infinitely rigid in the hypotheses formulated in §2.2.1.
The hull shown in figure 16 is obtained.

In particular, it is possible to deduce the expression (21) formalising respect for the worst case FC with thermomechanical behaviour in figure 10.

$$\begin{aligned} d_{\max} &\geq \varepsilon_{A,1,1/1,2thy}+\frac{t_{1,2}}{2}+\left(L_{1,2}+\frac{L_{2,1}}{2}\right)\times\left(\frac{t_{2,1}}{L_{2,1}}\right) \\ d_{\min} &\leq \varepsilon_{A,1,1/1,2thy}-\frac{t_{1,2}}{2}-\left(L_{1,2}+\frac{L_{2,1}}{2}\right)\times\left(\frac{t_{2,1}}{L_{2,1}}\right) \end{aligned} \qquad (21)$$

3- Application to a high-pressure turbine

3.1- Description of the turbine

The turbine consists of two sub-units: a rotor 12 and a stator (made up of parts numbered 1, 2, 3, 4, and 7) in a turning pair joint along **x** by means of ball bearings, numbered 13 and a cylindrical roller bearing, numbered 14: see figure 17. Part 12 has a revolution shape where the largest diameter corresponds to the diameter of the heads of the blades. Clearance at the top of blade between part 12 and part 1 of the stator is characterised by the difference in diameter between part 1 and part 12: see figure 17.

In order to maximise turbine power, this clearance should be minimised while ensuring that in all turbine operational phases part 12 does not touch part 1.

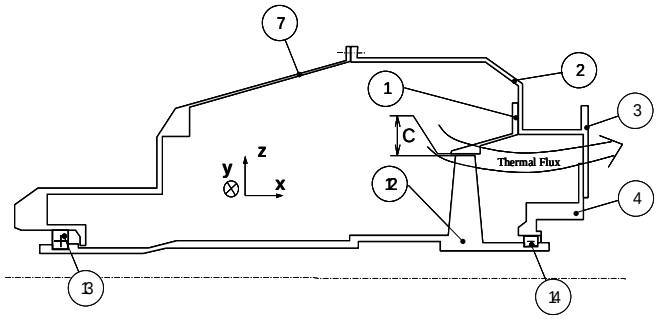

Figure 17 : Simplified geometric model of a high-pressure turbine.

When the turbine is operational, a flux of hot gases (about 1000 °C) is created in the combustion chamber (not shown in figure 17) and the consequence of this is to transform parts 1, 4 and 12 into thermomechanically deformable parts: see figure 17. In this application, the study is limited to a sub-unit of the turbine made up of parts 1 and 2: see figure 18.

The functional condition guaranteeing control of clearance C at the top of the blades between the rotor and the stator (see figure 17), corresponds to an FC for the alignment of the axes of surfaces 1,8 and 2,8: see figure 18.

FC is defined by equation (22) where e represents the distance between the axes of surfaces 1,8 and 2,8 following a direction orthogonal to the x-axis at point A:

$$e_{min} \leq e \leq e_{max} \qquad (22)$$

In this example, when the turbine is operational, only thermomechanical strains in part 1 will be taken into account. Part 2 is considered infinitely rigid and geometrically perfect: see figure 18.

The specifications required to satisfy the FC with two different behaviours have to be studied. In a first phase the turbine is modelled under rigid behaviour where only manufacturing defects and clearances in the different contacts will be taken into account. Next, the thermomechanical behaviour is considered where strains due to the flux of hot gases from the combustion chamber are integrated, at a point where the turbine is in stationary operating regime.

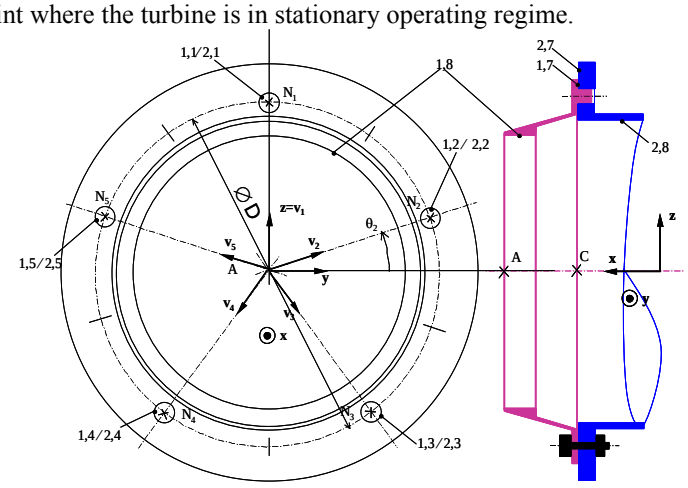

Figure 18 : Sub-unit of high-pressure turbine.

3.2- Rigid behaviour

3.2.1 Modelling 3D dimension chains of the turbine

Part 1 is placed in position by a support plane contact with part 2, via surfaces 1,7 and 2,7. Contacts between surfaces 1,1/2,1; 1,2/2,2; 1,3/2,3; 1,4/2,4; 1,5/2,5 modelled by ball and cylinder pair joints, complete the positioning between these two parts. Five clamping screws ensure that parts 1 and 2 are held in position. The graph of the joints corresponding to the system described in figure 18 is shown in figure 19 with the parameters of the different joints according to the model shown in §2.2.2.

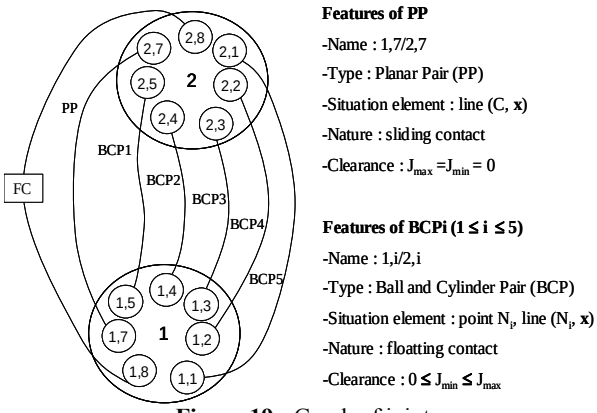

Figure 19 : Graph of joints.

Note the deviations in position between surfaces 1,8 and 2,8 by a small displacement torsor $\left[d_{1,8/2,8}\right]$. From the joint graph, the six relations that characterise the relative position of surfaces 1,8 and 2,8 are deduced:

$$\left\{\begin{array}{l}\left[d_{1,8/2,8}\right]=\left[d_{1,8/1,7}\right]+\left[d_{1,7/2,7}\right]+\left[d_{2,7/2,8}\right]\\ \left[d_{1,8/2,8}\right]=\left[d_{1,8/1,i}\right]+\left[d_{1,i/2,i}\right]+\left[d_{2,i/2,8}\right] \text{ with } i\in[1;5]\end{array}\right\} \quad (23)$$

Since part 2 is considered as infinitely rigid and without any geometric defect, torsors $\left[d_{2,7/2,7}\right]$ $\left[d_{2,i/2,8}\right] i\in[1;7]$ are null torsors. Equations (23) then become:

$$\left\{\begin{array}{l}\left[d_{1,8/2,8}\right]=\left[d_{1,8/1,7}\right]+\left[d_{1,7/2,7}\right]\\ \left[d_{1,8/2,8}\right]=\left[d_{1,8/1,i}\right]+\left[d_{1,i/2,i}\right] \text{ with } i\in[1;5]\end{array}\right\} \quad (24)$$

In part 1 it is necessary to control the displacement of surface 1,8 simultaneously in relation to surfaces 1,1 to 1,7. To do this, a system of AB references according to ISO standards is defined [I4], [I1] and [I3].
The plane surface 1,7 designated A is taken as primary reference and the group of five cylindrical surfaces (1,1 to 1,5) designated B is taken as a secondary reference: see figure 20. AB designates the system of references that make up primary reference A and secondary reference B.

As for part 1, the CD reference system is defined on part 2. The primary reference designated as C corresponds to surface 2,7. The secondary reference designated as D corresponds to the group of 5 surfaces 2,1 to 2,5.

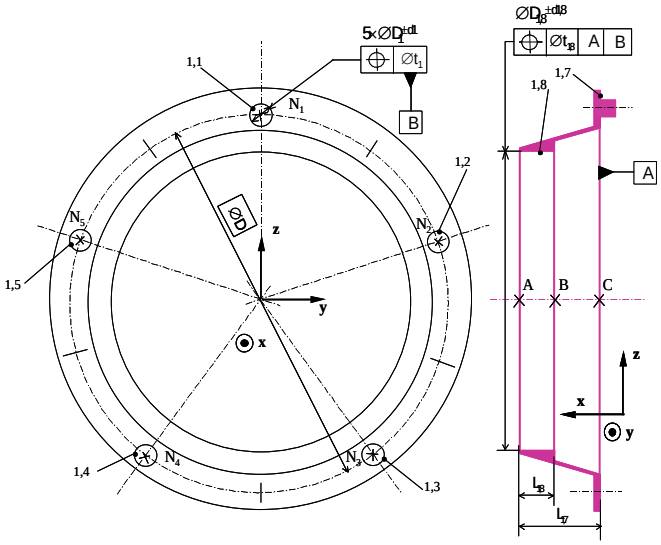

Figure 20 : Drawing showing definition of part 1.

The clearance hull characterising the displacement limits of surface 1,8 in relation to surface 2,8 is expressed by the following Minkowski sum:

$$\mathsf{D}_{1,8/2,8} = \mathsf{D}_{1,8/AB} + \mathsf{D}_{AB/CD} \qquad (25)$$

$\mathsf{D}_{1,8/AB}$ represents the deviation hull characterised by the location of surface 1,8 in relation to the reference system AB. $\mathsf{D}_{AB/CD}$ represents the clearance hull defined by the support plane joint (1,7/2,7) and the five ball and cylinder pair joints (1,i/2,i). Hull $\mathsf{D}_{AB/CD}$ is formalised by the intersection of the clearance hulls of the joint between surfaces 1,7/2,7 and the five joints 1,i/2,i:

$$\mathsf{D}_{AB/CD} = \mathsf{D}_{1,7/2,7} \cap \left(\mathsf{D}_{1,1/2,1} \cap \mathsf{D}_{1,2/2,2} \cap \mathsf{D}_{1,3/2,3} \cap \mathsf{D}_{1,4/2,4} \cap \mathsf{D}_{1,5/2,5}\right) \qquad (26)$$

3.2.2 Expression of the clearance hull between parts 1 and 2

For each slug the clearance is maximal: it corresponds to the difference between the maximum diameter of the hole and the minimum diameter of the shaft (cf. §2.1.1). Then the hull $\mathsf{D}_{1,i/2,i}$ at point N_i according to (27) is defined: see figure 21. This clearance is open in accordance with the four projections ρ_x, ρ_y, ρ_z et $\varepsilon_{N_i x}$. corresponding to the four degrees of freedom of a ball and cylinder pair joint.

$$\mathsf{D}_{1,i/2,i} = \left\{ \left(\boldsymbol{\varepsilon}_{Ni,1,i/2,i}.\mathbf{y}\right)^2 + \left(\boldsymbol{\varepsilon}_{Ni,1,i/2,i}.\mathbf{z}\right)^2 \le \left(\frac{J_{max}}{2}\right)^2 \right\} \qquad (27)$$

with $1 \le i \le 5$

Equation (28) deduces from (27) hull $\mathsf{D}_{1,i/2,i}$ expressed at point C by considering (29).

$$\mathsf{D}_{1,i/2,i} = \left\{ \begin{array}{l} \left(\varepsilon_{C,1,i/2,iy} - \frac{D}{2}\sin\theta_i.\rho_{1,i/2,ix}\right)^2 + \\ \left(\varepsilon_{C,1,i/2,iz} + \frac{D}{2}\cos\theta_i.\rho_{1,i/2,ix}\right)^2 \le \left(\frac{J_{max}}{2}\right)^2 \end{array} \right\} \qquad (28)$$

with $1 \le i \le 5$

$$\left\{ \begin{array}{l} \boldsymbol{\varepsilon}_{Ni,1,i/2,i} = \boldsymbol{\varepsilon}_{C,1,i/2,i} + \mathbf{N_i C} \times \boldsymbol{\rho}_{1,i/2,i} \\ \boldsymbol{\varepsilon}_{C,1,i/2,i} \begin{bmatrix} \varepsilon_{C,1,i/2,ix} \\ \varepsilon_{C,1,i/2,iy} \\ \varepsilon_{C,1,i/2,iz} \end{bmatrix}, \boldsymbol{\rho}_{1,i/2,i} \begin{bmatrix} \rho_{1,i/2,ix} \\ \rho_{1,i/2,iy} \\ \rho_{1,i/2,iz} \end{bmatrix} \text{ and } \mathbf{N_i C} \begin{bmatrix} 0 \\ -\frac{D}{2}\cos\theta_i \\ -\frac{D}{2}\sin\theta_i \end{bmatrix} \end{array} \right\} \qquad (29)$$

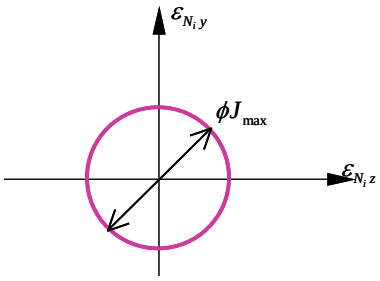

Figure 21 : Clearance hull $\mathsf{D}_{1,i/2,i}$.

The intersection of the five hulls $\mathsf{D}_{1,i/2,i}$ at point C is shown in figure 22. This hull is open according to projections in

ρ_y, ρ_z et ε_{Cx}. [GD1], [TD1] and [MD1].

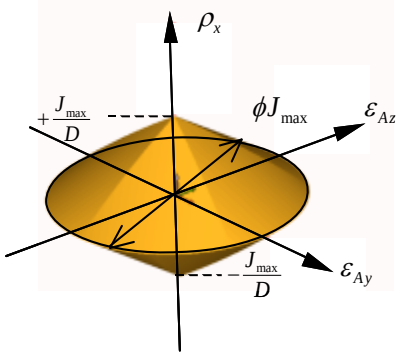

Figure 22 : Projected intersection according to ε_{Cy}, ε_{Cz}, ρ_x for the 5 hulls $D_{1,i/2,i}$.

By projecting this hull according to ρ_y and ε_{Cz} for $\rho_x = 0$ the hull described in figure 23 is obtained.
It can be seen that this hull remains invariant in relation to any translation orthogonal to the straight line $(A,\mathbf{x})$. It is axisymmetrical.

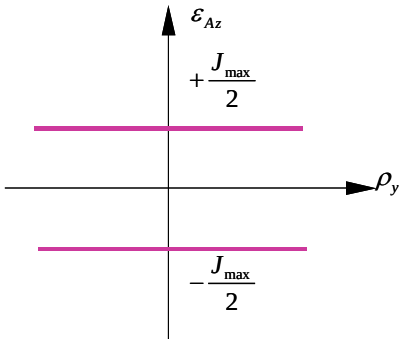

Figure 23 : Projected intersection according to ε_{Cz}, ρ_z for the 5 hulls $D_{1,i/2,i}$.

The planar pair between surfaces 1,7/2,7 suppresses rotations along y-axis and leaves translations along z-axis free.
Clearance in this joint is null.
Hull $D_{1,7/2,7}$ projected according to ε_{Cz}, ρ_z is shown in figure 24.

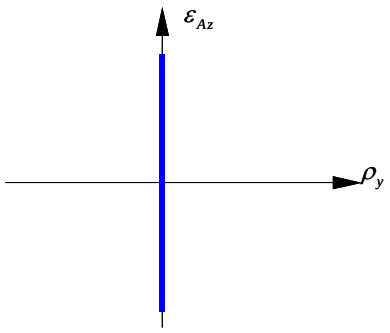

Figure 24 : Clearance hull of support plane joint.

The clearance hull $D_{AB/CD}$ defined by equation (26) is calculated and shown in figure 25. This is the intersection of clearance hull $D_{1,7/2,7}$ with the intersection of the 5 hulls $D_{1,i/2,i}$ at point C projected according to ε_{Cz}, ρ_z.
As ρ_y is null, the consequence is $\varepsilon_{Az} = \varepsilon_{Cz}$. The representation in figure 25 is also valid at point A.

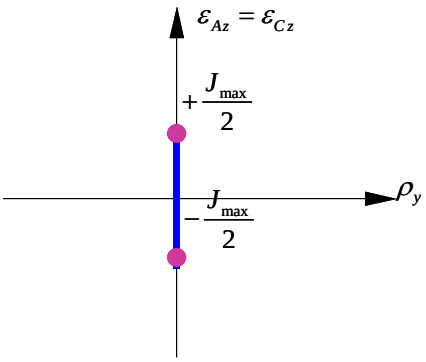

Figure 25 : Clearance hull.

3.2.3 Modelling the location of surface 1,8

By the same method as that presented in §2.1.3, the deviation hull $D_{1,8/AB}$ is defined at point A. This hull characterising the location specification (see figure 20) is shown in figure 26.

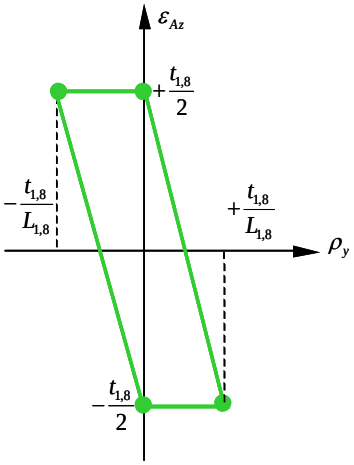

Figure 26 : Deviation hull of location of surface 1,8.

This hull remains invariant in relation to any translation orthogonal to the straight line $(A, \mathbf{x})$ given that the tolerance zone for the location specification is a cylinder [I1]. It is axisymmetrical.

3.2.4 Relations between functional condition, geometric specifications and contact specifications

The Minkowski sum defined by equation (25) is represented by figure 27.
In particular, expression (30) formalising respect for the worst case FC in rigid behaviour can be deduced.

$$\left.\begin{aligned} e_{max} &\geq +\frac{t_{1,8}}{2} + \frac{J_{max}}{2} \\ e_{min} &\leq -\frac{t_{1,8}}{2} - \frac{J_{max}}{2} \end{aligned}\right\} \qquad (30)$$

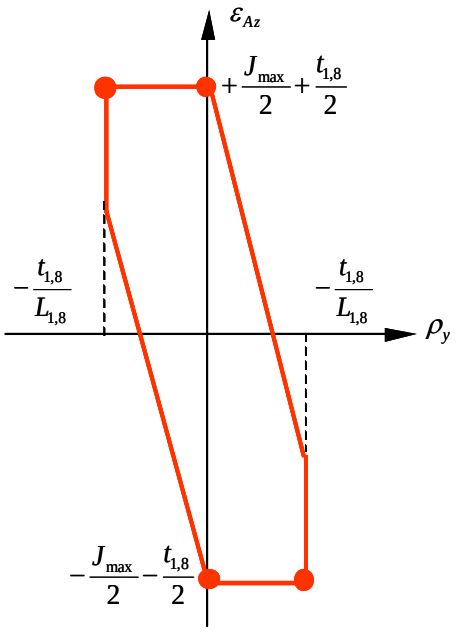

Figure 27 : Hull defining displacement limits of surface 1,8 in relation to surface 2,8 at point A.

3.3- Thermomechanical behaviour

The influence of the thermomechanical strains caused by a flux of gases from the combustion chamber will be modelled: see figure 17.

3.3.1 Integration of thermomechanical strains into the joints

As was described in §2.2.2, the nature of the contacts and the clearances can change under thermomechanical behaviour. Similarly, a contact may become a forced contact.
A preliminary thermomechanical study was carried out to determine changes in contacts. Thermal marginal conditions were provided by expert engineers working in the energy domain. They consisted of two fluxes: one convection flux due to hot gas from the combustion chamber, situated on the internal face of part 1 ; and convective cooling flux on the external face of part 1 : see figure 28.

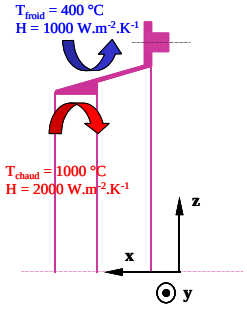

Figure 28 : Thermal marginal conditions.

As mechanical marginal conditions only contact conditions of the planar pair 1,7/2,7 are taken into account. This will enable first to analyse the behaviour of surfaces 1,1 to 1,5.
This first thermomechanical study shows that the radial displacement of the slugs is much greater than the maximal clearance present in each BCP type joint. A consequence is that the nature of the contact of the five ball and cylinder pair joints changes from floating to fixed.
Moreover, the strain on part 1 adds a forced contact to each BCP type joint according to direction $\mathbf{v}_i$: see figure 29.

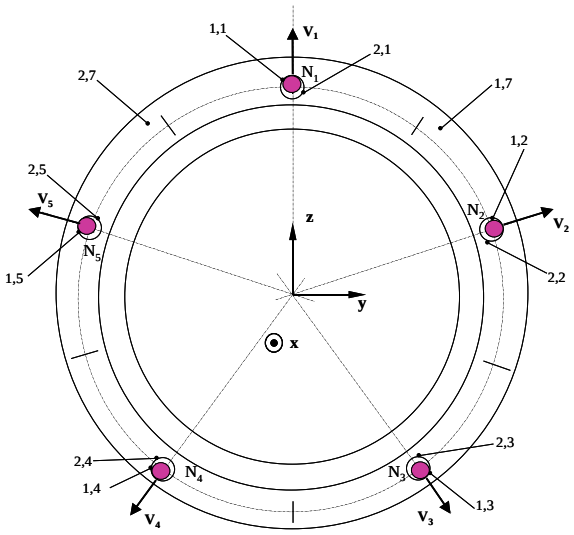

Figure 29 : Radial displacement of the slugs.

The clearance hull for each slug is therefore a point that corresponds to a null rotation and to a radial translation of J/2 in quantity (cf. §2.2.2 and figure 14).

The clearance hull $D_{AB/2,8}$ is a point centred on the origin given that slug distribution is angularly equidistant: see figure 30.

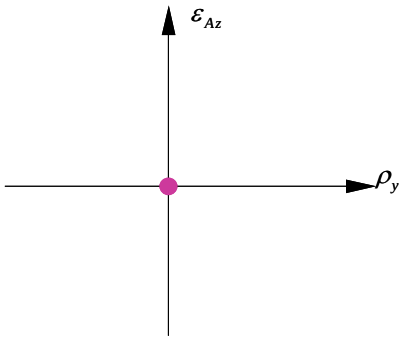

Figure 30 : Clearance hull of complete joint in two dimensions.

3.3.2 Integrating thermomechanical strains into the parts

A thermomechanical analysis of part 1 was carried out with the thermal marginal conditions defined in figure 28 and with mechanical marginal conditions that conformed to the parameters of the different joints under thermomechanical behaviour. Next, the geometry of surface 1,8 which was deformed by thermomechanical stresses has been studied. After analysing the deformed cylindrical surface the results for figures 31 and 32 using Samcef software have been obtained.

The deviations that derive from the thermomechanical stress on part 1 (see figure 31) give result (31) :

$$\left[d_{1,8/2,8}\right]_{th,A} = \begin{bmatrix} \boldsymbol{\rho}_{1,8,/2,8th} \\ \boldsymbol{\varepsilon}_{A,1,8,/2,8th} \end{bmatrix} \qquad (31)$$

with : $\boldsymbol{\rho}_{1,8,/2,8th} = \mathbf{0}$ and $\boldsymbol{\varepsilon}_{A,1,8,/2,8th} = \mathbf{0}$

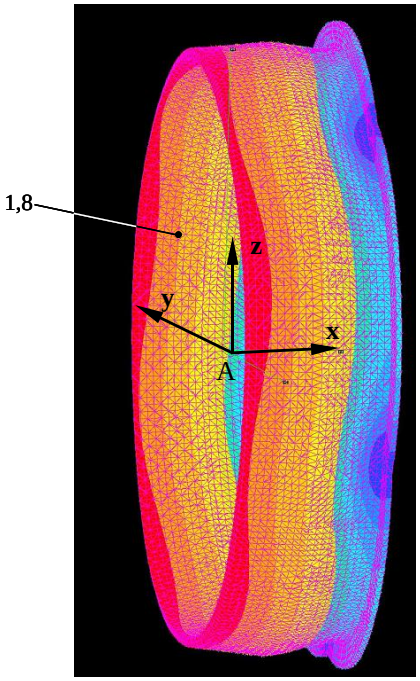

Figure 31 : Thermomechanical strain in part 1.

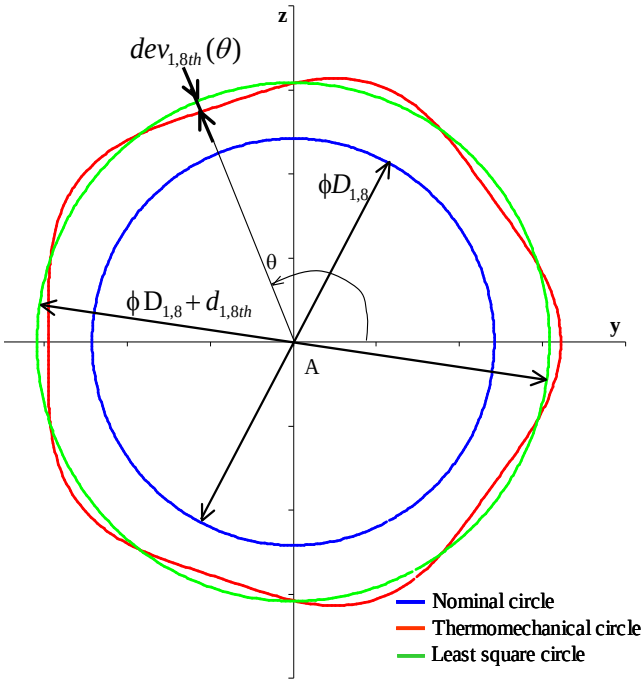

Figure 32 : Thermomechanical strain of surface 1,8 in plane $(A, \mathbf{x})$

The three following results in particular on the strain in plane $(A, \mathbf{x})$ have to be considered see figure 32:

- the translation deviation at point A in the centre of the least square circle in relation to the centre of the nominal circle: $\boldsymbol{\varepsilon}_{A,1,8/2,8th} = \mathbf{0}$
- the diameter of the least square circle of the section with the strain: $D_{1,8th} = D_{1,8} + d_{1,8th}$
- the form deviation of the section with the strain: $dev_{1,8th}(\theta)$

Figure 31 shows that the thermomechanical strain on surface 1,8 is not axisymmetrical.

Figure 33 shows hull $D_{1,8/2,8th}$ at point A in a process similar to that used in §2.2.3.

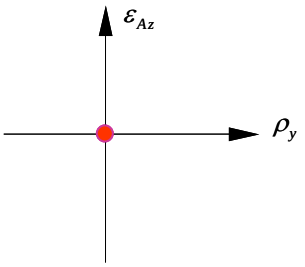

Figure 33 : Hull strain in surface 1,8 in relation to the nominal surface.

3.3.3 Synthesis: formalisation of relations between functional condition, geometric specifications and contact specifications

Using a similar method to that described in §2.2.4, based on relation (25), the Minkowski sum of hull $\mathrm{D}_{1,8/2,8}$ characterising the displacement limits for surface 1,8 in relation to surface 2,8 in relation to thermomechanical behaviour for the high pressure turbine can be calculated: see figure 34.
The strain on surface 1,8/2,8 is not axisymmetrical.

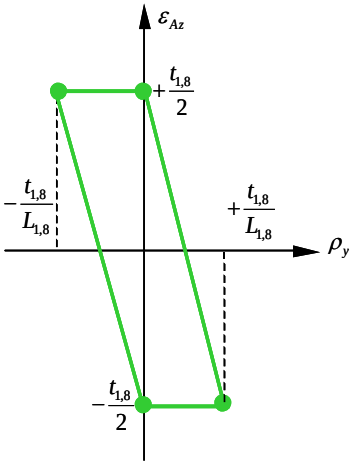

Figure 34 : Minkowski sum illustrating relation (25) with thermomechanical behaviour in figure 28.

In particular, from this expression (32) formalising respect for the worst case FC with thermomechanical behaviour is deduced.

$$\left.\begin{array}{l} e_{\max} \geq +\dfrac{t_{1,8}}{2} \\ e_{\min} \leq -\dfrac{t_{1,8}}{2} \end{array}\right\} \qquad (32)$$

It is also possible to determine the translation deviation $b_{1,8}(\theta)$ from a point on the cylindrical surface 1,8 in relation to its nominal position.
For rigid behaviour, equation (33) characterizes the translation deviation $b_{1,8}(\theta)$ and the limits of $\varepsilon_{A,1,8/2,8z}$ are given by the hull shown in figure 27.
For thermomechanical behaviour, equation (34) characterizes the translation deviation $b_{1,8}(\theta)$ and the limits of $\varepsilon_{A,1,8/2,8z}$ are given by the hull in figure 34.

$$b_{1,8}(\theta) = \varepsilon_{A,1,8/2,8z} + \frac{\mathrm{D}_{1,8} \pm d_{1,8}}{2} \qquad (33)$$

$$b_{1,8}(\theta) = \varepsilon_{A,1,8/2,8z} + \frac{\left(\mathrm{D}_{1,8} + d_{1,8th}\right) \pm d_{1,8}}{2} + dev_{1,8th}(\theta) \qquad (34)$$

The diameter deviation of cylindrical surface 1,8 defined by $\pm d_{1,8}$ (see figure 20, equations (33) and (34)) remains the same in rigid behaviour and thermomechanical behaviour.

4- Conclusions and future studies

This article shows how deviation hulls and clearance hulls can take thermomechanical strains into account in 3D dimension chains.
This paper demonstrated an application using a high pressure turbine from a helicopter engine.
For specific thermomechanical behaviour, thermomechanical strains are taken into account from a reference definition of the variability of geometrical defects corresponding to rigid behaviour.
Future work is centred on studying the distribution of geometrical defects arising from manufacturing dispersions and thermomechanical strains, for all behaviour modes of a turboshaft engine. As well as rigid behaviour, several different thermomechanical behaviours should be considered to represent the true operational cycle of a helicopter engine.
One of the main objectives of this study will be the possibility of proposing qualification criteria for the technical solutions envisaged in the design cycle of a high pressure turbine for helicopter engines assisted by geometric specifications.

Acknowledgements: We would like to thank Jean Luc Breining and Rainer Thomas from Turbomeca for their advice and technical assistance with this project.

5- References

[BB1] Bourdet P. and Ballot E. Geometrical behavior laws for computer aided tolerancing. In proc. of the 4th CIRP Seminar on Computer Aided Tolerancing, 1995.

[BM1] Ballu A. and Mathieu L. Choice of functional specifications using graphs within the frame work of education. In proc. of the 6th CIRP Seminar on Computer Aided Tolerancing ISBN 0-7923-5654-3, 197-206, Kluwer academic publisher, 1999.

[CB1] Clément A. and Bourdet, P. A Study of Optimal-Criteria Identification Based on the Small-Displacement Screw Model. Annals of the CIRP Vol. 37/1/1988, 1988.

[CR1] Clément A, Rivière A and Serre P. TTRS Declarative information model. In Proc of the 4th CIRP Seminar on Computer Aided Tolerancing, 1995.

[DB1] Dantan JY, Ballu A.and Mathieu L., Geometrical product specifications - model for product life cycle, Computer Aided Design; doi:10.1016/j.cad.2008.01.004, 2008.

[DE1] Defazio T.L., Edsall A. C., Gustavson R. E., Hernandez J., Hutchins P. M., Leung H. W., Luby S. C., Metsinger R. W., Nevins J. L., Tung K., Whitney D. E. A prototype of feature-based design for assembly. Journal of Mechanical Design, Vol. 115-4:723-734, 1993.

[DM1] Dantan JY, Mathieu L, Ballu A and Martin P., Tolerance synthesis: quantifier notion and virtual boundary. Computer Aided Design; 37:231-240, 2005.

[DT1] Dufaure J., Teissandier D., A tolerancing framework to support geometric specifications traceability, Int J Adv Manuf Technol, 36 (9-10): 894-907, 2008.

[F1] Fleming A., Geometric relationships between toleranced features. Artificial Intelligent; 37 :403-412, 1988.

[GD1] Giordano M. and Duret D. Clearance Space and Deviation Space, Application to three-dimensional chains of dimensions and positions, In proc. of the 3rd CIRP Seminar on Computer Aided Tolerancing, ISBN 2-212-08779-9, 179-196, Eyrolles, 1993.

[GS1] Giordano M., Samper S. and Petit J.P. Tolerance analysis and synthesis by means of deviation domains, axi-symetric cases. In proc. of the 9th CIRP Seminar on Computer Aided Tolerancing, ISBN 978-1-4020-5437-2, 85-94, Springer, 2005.

[I1] ISO 1101, Geometrical Product Specifications (GPS), Geometrical tolerancing, Tolerances of form, orientation, location and run-out, 2004.

[I2] ISO 3952-1, Kinematic diagrams - Graphical symbols- Part 1, 1981.

[I3] ISO 5459, Technical drawings - Geometrical tolerancing - Datums and datum-systems for geometrical tolerances, 1981.

[I4] ISO 8015, Technical drawings - Fundamental tolerancing principle, 1985.

[JC1] Jack Hu S. and Camelio J. Modeling and Control of Compliant Assembly Systems. CIRP Annals, Manufacturing Technology 55 (1):19-22, 2006.

[MD1] Mujezinovi A., Davidson JK. and Shah JJ. A new mathematical model for geometric tolerances as applied to round faces. ASME Transactions on Journal of Mechanical Design, 126:504–518, 2004.

[PT1] Pierre L., Teissandier D. and Nadeau J.P. Analyse des tolérances géométriques dans un contexte multi-expertises, application à une turbine de moteur d'hélicoptère, In proc. of CFM2007, 2007.

[RL1] Roy U and Li B. Representation and interpretation of geometric tolerances for polyhedral objects. Computer Aided Design;31(4):273–85, 1999.

[SC1] Stewart M. L. and Chase K. W. Variation simulation of fixtured assembly for compliant structures using piecewise-linear analysis. American Society of Mechanical Engineers, Manufacturing Engineering Division, MED Volume 16-1:591-600, 2005.

[SL1] Söderberg R., Lindkvist L. and Dahlström, S. Computer-aided robustness analysis for compliant assemblies. Journal of Engineering Design, 17:411 – 428, 2006.

[SS1] Shen Z., Shah J.J. and Davidson J.K. Analysis neutral data structure for GD&T. J Intell Manuf, DOI 10.1007/s10845-008-0096-2, 2008.

[T1] Turner J. U. Relative positionning of parts in assemblies using mathematical programming. Computer Aided Design, 22:394-400, 1990.

[TC1] Teissandier D., Couétard Y. and Gérard, A. A Computer Aided Tolerancing Model : Proportioned Assemblies Clearance Volume, Computer Aided Design, 31:805-817, 1999.

[TD1] Teissandier D., Delos V. and Couétard Y. Operations on polytopes: application to tolerance analysis In proc. of the 6th CIRP Seminar on Computer Aided Tolerancing ISBN 0-7923-5654-3, 425-433, Kluwer academic publisher, 1999.

[XW1] Xie K., Wells L., Camelio J. A. and Youn B. D. Variation propagation analysis on compliant assemblies considering contact interaction. Journal of Manufacturing Science and Engineering, Transactions of the ASME 129 (5):934-942, 2007.

[W1] Whitney D.E. and Adams J.D. Application of screw theory to analysis of mobility and constraint of mechanisms. Journal of mechanical design, 123:1:26-32, 2001.

[Z1] Ziegler, G. M.; Lectures on polytopes, ISBN 0-387-94365-X, Springer Verlag, 1995.